

Cancer Therapy

Selective Uptake of Cylindrical Poly(2-Oxazoline) Brush-AntiDEC205 Antibody-OVA Antigen Conjugates into DEC-Positive Dendritic Cells and Subsequent T-Cell Activation

Jasmin Bühler,^[a, b] Sabine Gietzen,^[a] Anika Reuter,^[a, c] Cinja Kappel,^[e] Karl Fischer,^[a] Sandra Decker,^[a] David Schäffel,^[d] Kaloian Koynov,^[d] Matthias Bros,^{*,[e]} Ingrid Tubbe,^[e] Stephan Grabbe,^{*,[c, e]} and Manfred Schmidt^{*,[a, b, c]}

Abstract: To achieve specific cell targeting by various receptors for oligosaccharides or antibodies, a carrier must not be taken up by any of the very many different cells and needs functional groups prone to clean conjugation chemistry to derive well-defined structures with a high biological specificity. A polymeric nanocarrier is presented that consists of a cylindrical brush polymer with poly(2-oxazoline) side chains carrying an azide functional group on each of the many side chain ends. After click conjugation of dye and an anti-DEC205 antibody to the periphery of the cylindrical brush polymer, antibody-mediated specific binding and uptake into DEC205⁺-positive mouse bone marrow-derived dendritic cells (BMDC) was observed, whereas binding and uptake by DEC205⁻ negative BMDC and non-DC was essentially absent. Additional conjugation of an antigen peptide yielded a multifunctional polymer structure with a much stronger antigen-specific T-cell stimulatory capacity of pretreated BMDC than application of antigen or polymer-antigen conjugate.

The ideal nanocarrier for biomedical applications is not cytotoxic, has a size between 10 and 100 nm, and does not form aggregates in blood serum that are due to strong interactions with the numerous proteins and enzymes present in the complex biological fluids.^[1] Poly(2-oxazoline)s are excellent candidates for this purpose,^[2] because they are known for their low cytotoxicity,^[3] biocompatibility,^[4,5] stealth behavior,^[6,7] and low protein adsorption from human blood.^[8]

Cylindrical polymer brushes have become increasingly popular because of their anisotropic character and the recent results on shape dependent endocytosis.^[9–12] Furthermore, polymeric brushes may offer a multiplicity of functional groups which are advantageous for conjugation of biologically active compounds.

Several publications report cylindrical brushes with poly(2-oxazoline) side chains prepared by “grafting from”^[13,14] and “grafting through”^[15–17] techniques. Recently our group published the synthesis of cylindrical brushes with poly(2-isopropyl-2-oxazoline) side chains by grafting through with unprecedented high main chain degrees of polymerization.^[18] All of the cylindrical brushes with poly(2-oxazoline) side chains reported to date do not contain functional groups for further conjugation experiments except for one work in which functionalized polymers were prepared though with a main-chain degree of polymerization as low as only 13.^[19] However, azide functionalized linear poly(2-oxazoline)s have been described.^[20–24]

To assess the suitability of the cylindrical brushes described herein to serve as nanocarriers for immuno-therapeutic approaches, their binding and uptake by DC was analyzed, because DC represent an important immune cell population. In their activated state, DC constitute the most potent antigen-presenting cells of the immune system that are solely able to initiate primary immune responses.^[25] Of the several DC subpopulations known, CD8⁺ DC that co-express the C-type lectin receptor DEC205 bear the highest potential to activate cytotoxic T lymphocytes.^[26] Conjugation of anti-DEC205 with antigen and adjuvant resulted in partial loss of targeting activity,^[27] whereas conjugation of an antigen only was shown to main-

[a] Dr. J. Bühler,⁺ S. Gietzen,⁺ Dr. A. Reuter, Dr. K. Fischer, S. Decker, Dr. M. Schmidt
Institute for Physical Chemistry, University of Mainz
Jakob-Welder Weg 11, 55099 Mainz (Germany)
E-mail: mschmidt@uni-mainz.de

[b] Dr. J. Bühler,⁺ Dr. M. Schmidt
Graduate School Materials Science
Staudinger Weg 9, 55128 Mainz (Germany)

[c] Dr. A. Reuter, Dr. S. Grabbe, Dr. M. Schmidt
Max Planck Graduate Center
Staudinger Weg 9, 55128 Mainz (Germany)

[d] D. Schäffel, Dr. K. Koynov
Max Planck Institute for Polymer Research
Ackermannweg 10, 55128 Mainz (Germany)

[e] C. Kappel, Dr. M. Bros, I. Tubbe, Dr. S. Grabbe
Department of Dermatology
University Medical Center of the Johannes Gutenberg
University Mainz
Langenbeckstrasse 1, 55131 Mainz (Germany)
E-mail: mbros@uni-mainz.de
stephan.grabbe@unimedizin-mainz.de

[⁺] These authors contributed equally to this work.

Supporting information for this article is available on the WWW under <http://dx.doi.org/10.1002/chem.201403942>.

tain DEC205 receptor mediated binding and uptake of antigen by this DC subpopulation.^[28,29]

Polymer–antibody rather than polymer–antibody fragment conjugates are less frequently reported.^[30–32] Antithymocyte globuline,^[33] polyclonal human immunoglobulin, and monoclonal anti-RAGE antibody^[34] were successfully conjugated to linear flexible hydroxypropylmethacrylate (HPMA) chains with no or little loss of antibody activity. Also polymeric capsules of a few μm in size were decorated by a few hundred thousand humanized A33 monoclonal antibodies were reported to selectively address human colorectal cancer cells.^[35,36]

Herein, the binding and uptake properties of bare cylindrical brushes were investigated in comparison to cylindrical brushes conjugated with a DEC205-specific antibody, when co-incubated with DC.

The synthesis is summarized in Scheme 1. The synthesis of the azide-functionalized poly(2-oxazoline) macromonomers was performed similar to the poly(2-isopropyl-2-oxazoline) macromonomer synthesis published recently^[18] and is described in some detail in the Supporting Information. Three different azide-functionalized macromonomers were synthesized and characterized by NMR and IR spectroscopy, GPC, and MALDI-TOF spectrometry (Supporting Information, Figures S1–S11). The results are summarized in Table 1.

Table 1 reveals the molar masses determined by MALDI-TOF and NMR to be similar. The ratio of the 2-ethyl-2-oxazoline block to 2-isopropyl-2-oxazoline block of the N_3 -poly(2-ethyl-2-isopropyl-2-oxazoline) macromonomer was determined by ^1H NMR to be 60% to 40%. MALDI-TOF was not measured for the block co-macromonomer as there would be different distri-

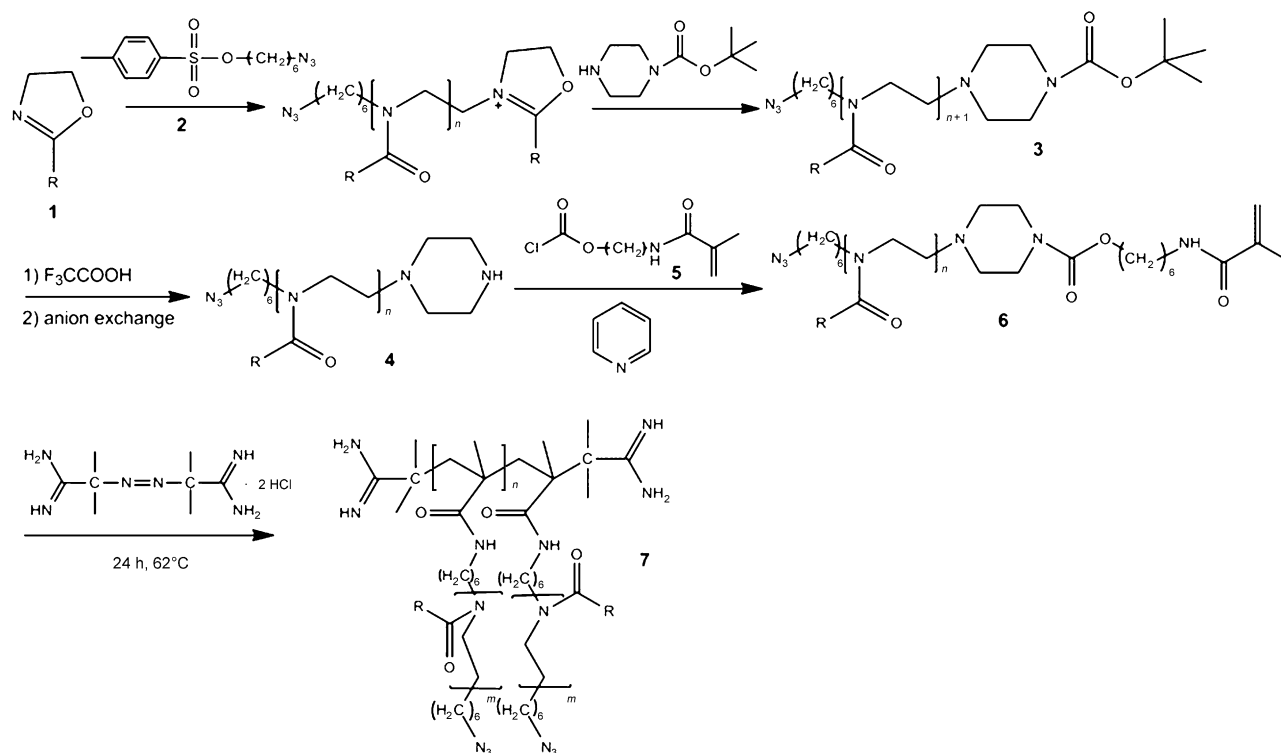
Table 1. Characterization of the macromonomers.			
	N_3 -PiPrOx	N_3 -PEtOx	N_3 -PEtOx-b-PiPrOx
M_w/M_n (MALDI/GPC)	1.12/1.13	1.20/1.16	–/1.1
M_n (MALDI) [g mol^{-1}]	4707	3623	–
M_n (GPC) [g mol^{-1}]	14800 ^[a]	13400 ^[a]	18900*
M_n (^1H NMR) [g mol^{-1}]	4946	3694	5869
M_w (MALDI) [g mol^{-1}]	5292	4330	–
P_n	40	33	61

[a] GPC with PMMA calibration yields values that are too large.

butions owing to the different block lengths. For further discussion we will use the ^1H NMR-determined molar masses.

All the three azide-functionalized macromonomers were polymerized in highly concentrated aqueous solutions at 62°C . The IR spectra of all azide end-functionalized brushes show the characteristic band at 2100 cm^{-1} (Supporting Information, Figure S12). After reduction with tris(2-carboxyethyl)phosphine, the azide bands disappeared (Supporting Information, Figure S13).

Polymerization of block co-macromonomers leads to core-shell cylindrical brushes;^[37] that is, polymerization of N_3 -poly(2-ethyl-2-isopropyl-2-oxazoline) macromonomers yields a core-shell structure with a core consisting of slightly hydrophobic poly(2-isopropyl-oxazoline) chains and a corona of hydrophilic poly(2-ethyl-oxazoline) chains. Representative DLS and SLS measurements of the cylindrical brushes with N_3 -poly(2-ethyl-2-isopropyl-2-oxazoline) side chains are shown in Figure 1 (for Zimm plots of the other cylindrical bushes, see the Supporting



Scheme 1. Synthesis of azide-functionalized poly(2-oxazoline)s.

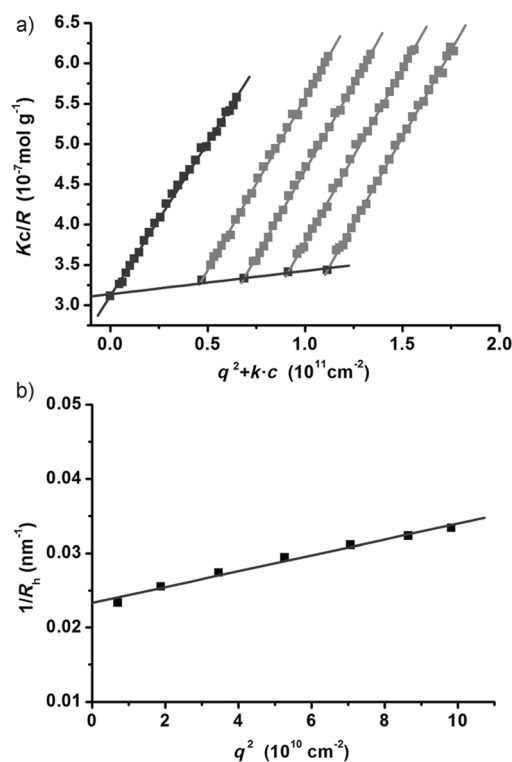


Figure 1. a) Zimm plot and b) reciprocal hydrodynamic radius of the azide end-functionalized cylindrical core-shell brush N_3 -poly(2-ethyl-block-2-isopropyl-2-oxazoline) in methanol with 5 mM added LiBr at 20 °C.

Table 2. Light scattering characterization including the degree of polymerization P_w of the azide end-functionalized brush polymers with poly(2-oxazoline) side chains.

	R_g [nm]	R_h [nm]	$\rho = R_g/R_h$	M_w (LS) [g mol ⁻¹]	dn/dc [cm ³ g ⁻¹]	P_w (LS)	M_w/M_n (GPC)
N_3 -PiPrOx-brush	37.4	26	1.44	$1.3 \cdot 10^6$	0.163	254	2.2
N_3 -PEtOx-brush	32.3	21	1.54	$6.2 \cdot 10^5$	0.177	167	1.7
N_3 -PEtOx- <i>b</i> -PiPrOx-brush	60.5	42	1.44	$3.2 \cdot 10^6$	0.177	547	2.4

Information, Figure S14). The results are summarized in Table 2. GPC calibrated by PMMA standards revealed polydispersities $M_w/M_n \approx 2$ for all samples, as expected (Supporting Information, Figure S11).

AFM (Figure 2; Supporting Information, Figure S15) illustrates the expected worm-like structures in qualitative agreement with the results obtained by static and dynamic light scattering. The N_3 -poly(2-ethyl-2-oxazoline) brush shows besides worm-like structures a multiplicity of spherical particles resulting in the much lower molecular weight compared to the other two brushes.

None of the cylindrical brush polymers exerted inhibitory effects on the metabolic activity of both human HEK293 and mouse BMDCs to any cell-type specific extent, that is, the 50% cell survival concentration was determined to be well above $1 \mu\text{g} \mu\text{L}^{-1}$ (Supporting Information, Table S3).

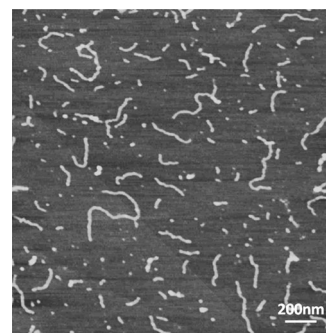


Figure 2. AFM image (height) of azide end-functionalized core-shell poly(2-oxazoline) brush N_3 -poly(2-ethyl-block-2-isopropyl-2-oxazoline) spin-cast onto mica from aqueous solution at $c = 0.1 \text{ g L}^{-1}$.

Recently our group developed a method that allows the determination of aggregation behavior of nanoparticles in human blood serum by dynamic light scattering.^[38] The correlation function of nanoparticles or polymers in serum solution, $g_1(t)_{\text{mix}}$ should be well-fitted the adequate weighted sum of known correlation functions measured from the polymer in isotonic solution, $g_1(t)_p$ and of undiluted serum, $g_1(t)_s$:

$$g_1(t)_{\text{mix}} = a_p g_1(t)_p + a_s g_1(t)_s + (a_A g_1(t)_A) \quad (1)$$

where a_p and a_s represent the amplitudes as the only fit parameters.

In the case of aggregation, a third correlation function describing the aggregate, $g_1(t)_A$, has to be added:

$$g_1(t)_{\text{mix}} = a_p g_1(t)_p + a_s g_1(t)_s + a_A g_1(t)_A \quad (2)$$

Figure 3 shows the autocorrelation function of the mixture of serum and N_3 -PiPrOx brush (a) as well as the mixture of serum and N_3 -PEtOx-*b*-PiPrOx brush (b). For the latter sample, the data points of the mixture are well-described by the force fit with the sum of individual correlation functions of serum and polymer brush, meaning no or negligible aggregation has taken place. Similar results were obtained for the N_3 -PEtOx brush (data not shown).

In contrast, the autocorrelation function of the mixture of serum and N_3 -PiPrOx-brush could not be perfectly fitted by the force fit with the sum of individual correlation functions of serum and polymer brush (Eq. (1); Figure 3 black line). A third correlation function is necessary to achieve a perfect fit (Eq. (2); Figure 3, gray line) and indicates a significant amount of aggregates of 360 nm radius to be present, which may be caused by the higher hydrophobicity of the N_3 -PiPrOx-brush. Hydrophobic proteins such as lipoproteins may interact with the polymer brush, leading to aggregation, although the extent of aggregation is quite small in view of the "intensity weighting" of DLS.

The data above reveal that the N_3 -EtOx and the N_3 -PEtOx-*b*-PiPrOx brushes do not form aggregates in concentrated blood serum, which could provoke unwanted uptake by macrophages and negatively influence the circulation time for later in vivo experiments.

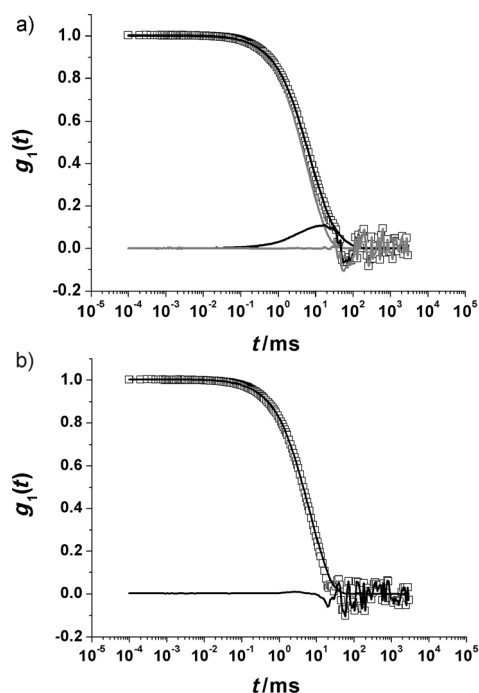


Figure 3. Autocorrelation functions of a) N_3 -PiPrOx and b) N_3 -PEtOx-*b*-PiPrOx brushes in human blood serum; gray lines represent the force fits with the sum of the individual correlation functions of serum and polymer brush according to Eq. (1); black lines represent the fits according to Eq. (2) accounting for the presence of aggregates; scattering angle 30° .

Dibenzocyclooctyne-modified antiDEC205 antibody was conjugated to the N_3 -poly(2-ethyl-2-isopropyl-2-oxazoline) brush utilizing copper-free 1–3 dipolar cycloaddition chemistry (Supporting Information, Scheme S2).^[39] According to UV/Vis spectroscopy, approximately 8 to 10 antibodies were bound to one cylindrical brush polymer (Supporting Information, Figure S17). No free antibody could be detected in the conjugate by gel electrophoresis (Supporting Information, Figure S18).

Fluorescence-activated cell sorting (FACS) showed that 29% of the $CD11^+$ BMDC population co-expressed DEC205, while 33% of the $CD11^+$ BMDC populations lacked DEC205 expression, and 37% of the cells were $CD11^-$ negative; that is, were no DCs (Figure 4a). The mean fluorescence intensity (MFI) of either $CD11^+$ BMDC population as well as of non-DC co-incubated with N_3 -PEtOx-*b*-PiPrOx-brushes for 4 h was rather low, as shown by the dotted lines in Figure 4b–d. When co-incubated with the polymer–antibody conjugate, a three-fold higher MFI was observed for $DEC205^+CD11^+$ BMDC (solid line in Figure 4b). In contrast, neither $DEC205^-CD11^+$ BMDC nor non-DC showed any considerable increase in polymer binding (solid lines in Figure 4c,d). Confocal laser scanning microscopy (CLSM) images confirmed this result and revealed polymer and antibody to be co-localized inside of $DEC205^+CD11^+$ BMDCs (Figure 4e,f). The corresponding FACS data and CLSM pictures for BMDC co-incubated with unconjugated polymer brushes are given in the Supporting Information, Figure S21.

After 4 h, 73% of the $DEC205^+$ BMDCs had engaged conjugate. It should be noted that cellular engagement of polymer antibody conjugates was blocked, if the BMDCs were incubat-

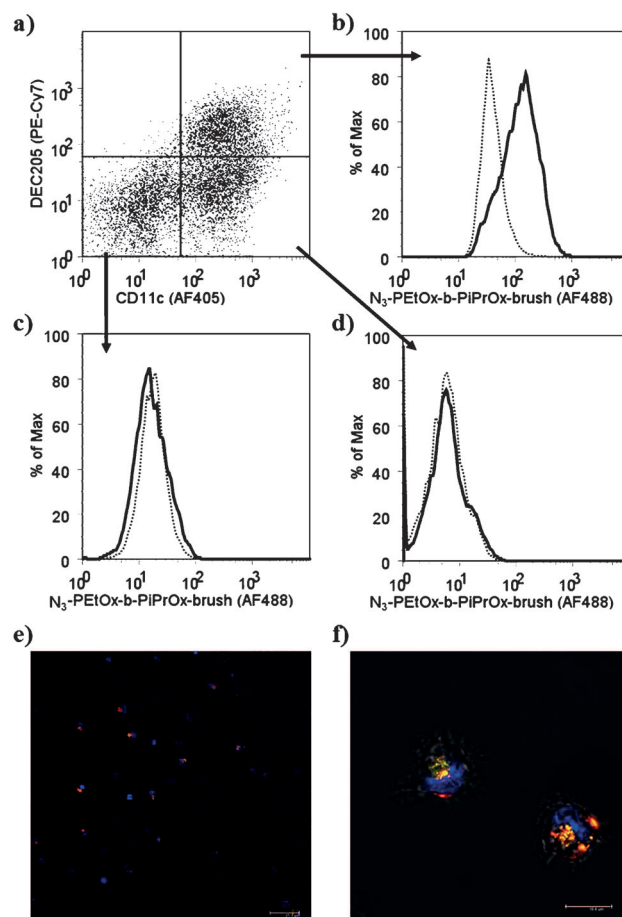


Figure 4. Binding and uptake of N_3 -poly(2-ethyl-block-2-isopropyl-2-oxazoline) brush-antiDEC205 conjugates by BMDC. Unstimulated BMDC were co-incubated for 4 hours in parallel with Carboxy-Rhodamine110-labeled N_3 -PEtOx-*b*-PiPrOx-brush, unconjugated or conjugated with anti-DEC205 antibody (10^{12} particles per 5×10^5 cells). a) BMDCs were double-stained with DEC205 and CD11c specific antibodies. The dot plot shows the distribution of the different subpopulations of BMDC co-incubated with anti-DEC205 antibody conjugated polymer. b)–d) Curves show different evaluations of one experiment and indicate cellular binding of anti-DEC205 antibody conjugated (thick solid line) and unconjugated polymer (thin dotted line) by the different cell populations. The corresponding MFI are given in brackets: b) $CD11c^+DEC205^+$ (MFI: 152.6 versus 44.6), c) $CD11c^+DEC205^-$: (MFI: 20.1 vs. 19.5), and d) $CD11c^-$ non-DCs (MFI: 8.1 vs. 7.2). Graphs are representative of 10 experiments. e), f) CLSM pictures of the polymer-DEC205 conjugates taken up by DCs. The polymer is labeled by Carboxyrhodamin (green), the DEC205 by AF647 (red). The orange color shows superposition of polymer and DEC205, that is, the intact conjugate. Hoechst 33342 (blue) was utilized to label cell nuclei. Scale bars 25.3 μm (e) and 10.6 μm (f).

ed with native anti-DEC205 antibody at large excess prior to addition of polymer antibody conjugates (Supporting Information, Figure S22).

To demonstrate a potential biological application of the cylindrical brush conjugates, the SIINFEKL-sequence of the OVA-antigen was additionally conjugated to the cylindrical brush polymer. As described in detail in the Supporting Information, Scheme S3, the AF546-labeled C-SGLEQLE-SIINFEKL oligopeptide (AG, derived from the ovalbumine antigen) was conjugated to the N_3 -poly(2-ethyl-block-2-isopropyl-2-oxazoline) cylindrical brush (CB) first, followed by conjugation of DBCO-func-

tionalized anti-DEC205 antibody (sample CB-AG-aDEC205). The trailer sequence SGLEQLE is known to be enzymatically cleavable by cells^[40] and cysteine was added for the conjugation reaction. On average, the final conjugate contained 17 antigen fragments and 7.5 anti-DEC205 molecules (Supporting Information, Figures S19 and S20).

The suitability of CB-AG-aDEC205 to confer efficient uptake of antigen into BMDCs was monitored by a proliferation of peptide (or SIINFEKL) reactive CD8⁺ T-cells. As shown in Figure 5, BMDC pre-incubated for 4 h with the CB-AG-aDEC205 conjugate (no. 4) induced much stronger proliferation of sub-

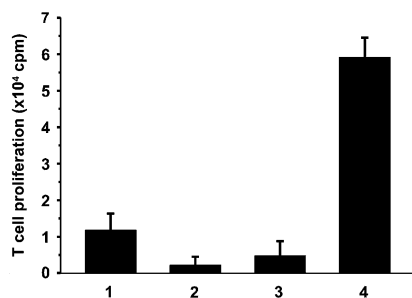


Figure 5. Antigen-specific CD8⁺ T-cell stimulatory capacity of BMDCs pre-incubated with the cylindrical brush conjugate CB-AG-aDEC205. In parallel assays, unstimulated BMDCs (each 5×10^5 cells) were incubated for 4 h with C-SGLEQLE-SIINFEKL peptide (1), with non-conjugated N3-poly(2-ethyl-block-2-isopropyl-2-oxazoline cylindrical brushes (2), with cylindrical brush-antigen conjugate (3), and with CB-AG-aDEC205 carrying both aDEC205 and C-SGLEQLE-SIINFEKL (4), at equimolar concentration of antigen (no. 1, 3, and 4: 10^{12} peptide molecules) or equal number of cylindrical brush polymer chains (no. 2 and 4).

sequently co-cultured peptide-reactive CD8⁺ T-cells than BMDCs pretreated with either antigen alone (no. 1) or polymer-antigen conjugate without aDEC205 (no. 3). The cylindrical brush polymer alone served as a negative control (no. 2).

Thus the azide functionalized polymer brushes with 2-ethyl-2-oxazoline and 2-ethyl-block-2-isopropyl-2-oxazoline side chains seem to be promising candidates for the application as nanocarriers for an antibody mediated specific targeting of cells as it is used in the immune cancer therapy.^[41–45] Although biodegradable the particles utilized so far were spherical in shape with sizes well above 100 nm up to 1 μ m. Thus, they might be taken up by macrophages by unspecific phagocytosis. Although the presented polymer brushes also exhibit high molar masses (Table 2) it should be noted that size rather than molar mass should be the relevant property for body circulation and recognition by macrophages. In this respect, the small size of the cylindrical brush polymers well below 100 nm in combination with their anisotropic shape makes them interesting candidates to study in vivo distribution in future experiments. As compared to antibody conjugates with antigen and/or adjuvant as reported recently^[27–29] the very large number of chemically accessible functional groups (that is, more than 100 azide groups per polymer) may allow particles to be produced with ten and more antibodies which may enhance cell-type-specific targeting.^[27] Furthermore, these particles may contain

several tens of antigen and/or adjuvant molecules to yield a higher quantity of cargo delivered on a per cell base. The applied click chemistry yields almost quantitative conjugation results and allows for the attachment of a predictable number of even different peptide antigens, which may serve to induce both CD4⁺ and CD8⁺ T-cell responses at the same time. Likewise, conjugation with different adjuvants that trigger distinct signaling pathways may serve to exert synergistic effects in terms of DC activation, and therefore the extent of subsequent T-cell stimulation.^[46]

Acknowledgements

Financial support by the DFG graduate school MAINZ (J.B.), by the Max Planck Graduate Center, Mainz, and by the German Science Foundation (SFB625, SFB1066) is gratefully acknowledged. CLSM measurements were performed at the Institute for Molecular Biology, Mainz. Some dye labeling experiments were conducted by Meike Schinnerer, Institute of Physical Chemistry, University Mainz, which is gratefully acknowledged.

Keywords: brush polymers · cancer therapy · dendritic cells · nanocarriers · T-cells

- [1] D. Weller, A. Medina-Oliva, H. Claus, S. Gietzen, K. Mohr, A. Reuter, D. Schäffel, S. Schöttler, K. Koynov, M. Bros, *Macromolecules* **2013**, *46*, 8519–8527.
- [2] R. Luxenhofer, Y. Han, A. Schulz, J. Tong, Z. He, A. V. Kabanov, R. Jordan, *Macromol. Rapid Commun.* **2012**, *33*, 1724.
- [3] R. Luxenhofer, G. Sahay, A. Schulz, D. Alakhova, T. K. Bronich, R. Jordan, A. V. Kabanov, *J. Controlled Release* **2011**, *153*, 73–82.
- [4] P. Goddard, L. E. Hutchinson, J. Brown, L. J. Brookman, *J. Controlled Release* **1989**, *10*, 5–16.
- [5] F. C. Gaertner, R. Luxenhofer, B. Blechert, R. Jordan, M. Essler, *J. Controlled Release* **2007**, *119*, 291–300.
- [6] M. C. Woodle, C. M. Engbers, S. Zalipsky, *Bioconjugate Chem.* **1994**, *5*, 493–496.
- [7] S. Zalipsky, C. B. Hansen, J. M. Oaks, T. M. Allen, *J. Pharm. Sci.* **1996**, *85*, 133–137.
- [8] R. Konradi, B. Pidhatika, A. Mühlebach, M. Textor, *Langmuir* **2008**, *24*, 613–616.
- [9] Y. Geng, P. Dalhaimer, S. Cai, R. Tsai, M. Tewari, T. Minko, D. E. Discher, *Nat. Nano* **2007**, *2*, 249–255.
- [10] J. Champion, S. Mitragotri, *Pharm. Res.* **2009**, *26*, 244–249.
- [11] S. Cai, K. Vijayan, D. Cheng, E. Lima, D. Discher, *Pharm. Res.* **2007**, *24*, 2099–2109.
- [12] J. L. Perry, K. G. Reuter, M. P. Kai, K. P. Herlihy, S. W. Jones, J. C. Luft, M. Napier, J. E. Bear, J. M. DeSimone, *Nano Lett.* **2012**, *12*, 5304–5310.
- [13] N. Zhang, S. Huber, A. Schulz, R. Luxenhofer, R. Jordan, *Macromolecules* **2009**, *42*, 2215–2221.
- [14] N. Zhang, R. Luxenhofer, R. Jordan, *Macromol. Chem. Phys.* **2012**, *213*, 1963–1969.
- [15] C. Weber, C. Remzi Becer, W. Guenther, R. Hoogenboom, U. S. Schubert, *Macromolecules* **2009**, *42*, 160–167.
- [16] C. Weber, A. Krieg, R. M. Paulus, H. M. L. Lambermont-Thijs, C. R. Becer, R. Hoogenboom, U. S. Schubert, *Macromol. Symp.* **2011**, *308*, 17–24.
- [17] C. Weber, S. Rogers, A. Vollrath, S. Hoepfener, T. Rudolph, N. Fritz, R. Hoogenboom, U. S. Schubert, *J. Polym. Sci. A: Polym. Chem.* **2013**, *51*, 139–148.
- [18] J. Bühler, S. Muth, K. Fischer, M. Schmidt, *Macromol. Rapid Commun.* **2013**, *34*, 588–594.
- [19] C. Weber, J. A. Czaplewski, A. Baumgaertel, E. Altuntas, M. Gottschaldt, R. Hoogenboom, U. S. Schubert, *Macromolecules* **2012**, *45*, 46–55.

- [20] G. Volet, T.-X. Lav, J. Babinot, C. Amiel, *Macromol. Chem. Phys.* **2011**, *212*, 118–124.
- [21] W. H. Binder, H. Gruber, *Macromol. Chem. Phys.* **2000**, *201*, 949–957.
- [22] T.-X. Lav, P. Lemechko, E. Renard, C. Amiel, V. Langlois, G. Volet, *React. Funct. Polym.* **2013**, *73*, 1001–1008.
- [23] C. Guis, H. Cheradame, *Eur. Polym. J.* **2000**, *36*, 2581–2590.
- [24] K. Kempe, R. Hoogenboom, M. Jaeger, U. S. Schubert, *Macromolecules* **2011**, *44*, 6424–6432.
- [25] O. Joffre, M. A. Nolte, R. Spörri, C. R. e. Sousa, *Immunol. Rev.* **2009**, *227*, 234–247.
- [26] P. M. Domínguez, C. Ardavín, *Immunol. Rev.* **2010**, *234*, 90–104.
- [27] M. Kreutz, B. Giquel, Q. Hu, R. Abuknesha, S. Uematsu, S. Akira, F. O. Nestle, S. S. Diebold, *PLoS ONE* **2012**, *7*, e40208 EP.
- [28] L. Bonifaz, D. Bonnyay, K. Mahnke, M. Rivera, M. C. Nussenzweig, R. M. Steinman, *J. Exp. Med.* **2002**, *196*, 1627–1638.
- [29] T. S. Johnson, K. Mahnke, V. Storn, K. Schönfeld, S. Ring, D. M. Nettelbeck, H. J. Haisma, F. Le Gall, R. E. Kontermann, A. H. Enk, *Clin. Cancer Res.* **2008**, *14*, 8169–8177.
- [30] M. C. Garnett, *Adv. Drug Delivery Rev.* **2001**, *53*, 171–216.
- [31] J. Kopeček, P. Kopečková, *Adv. Drug Delivery Rev.* **2010**, *62*, 122–149.
- [32] J. Kopeček, *Adv. Drug Delivery Rev.* **2013**, *65*, 49–59.
- [33] K. Ulbrich, T. Etrych, P. Chytil, M. Jelínková, B. Říhová, *J. Controlled Release* **2003**, *87*, 33–47.
- [34] K. Tappertzhofen, V. V. Metz, M. Hubo, M. Barz, R. Postina, H. Jonuleit, R. Zentel, *Macromol. Biosci.* **2013**, *13*, 203–214.
- [35] A. P. R. Johnston, M. M. J. Kamphuis, G. K. Such, A. M. Scott, E. C. Nice, J. K. Heath, F. Caruso, *ACS Nano* **2012**, *6*, 6667–6674.
- [36] M. M. J. Kamphuis, A. P. R. Johnston, G. K. Such, H. H. Dam, R. A. Evans, A. M. Scott, E. C. Nice, J. K. Heath, F. Caruso, *J. Am. Chem. Soc.* **2010**, *132*, 15881–15883.
- [37] R. Djalali, N. Hugenberg, K. Fischer, M. Schmidt, *Macromol. Rapid Commun.* **1999**, *20*, 444–449.
- [38] K. Rausch, A. Reuter, K. Fischer, M. Schmidt, *Biomacromolecules* **2010**, *11*, 2836–2839.
- [39] E. M. Sletten, C. R. Bertozzi, *Acc. Chem. Res.* **2011**, *44*, 666–676.
- [40] R. J. Binder, P. K. Srivastava, *Proc. Natl. Acad. Sci. USA* **2004**, *101*, 6128–6133.
- [41] Y. J. Kwon, E. James, N. Shastri, J. M. J. Fréchet, *Proc. Natl. Acad. Sci. USA* **2005**, *102*, 18264–18268.
- [42] A. Bandyopadhyay, R. L. Fine, S. Demento, L. K. Bockenstedt, T. M. Fahmy, *Biomaterials* **2011**, *32*, 3094–3105.
- [43] A. C. Shirali, M. Look, W. Du, E. Kassis, H. W. Stout-Delgado, T. M. Fahmy, D. R. Goldstein, *Am. J. Transplant.* **2011**, *11*, 2582–2592.
- [44] J. Park, W. Gao, R. Whiston, T. B. Strom, S. Metcalfe, T. M. Fahmy, *Mol. Pharm.* **2011**, *8*, 143–152.
- [45] L. J. Cruz, P. J. Tacken, F. Bonetto, S. I. Buschow, H. J. Croes, M. Wijers, I. J. de Vries, C. G. Figdor, *Mol. Pharm.* **2011**, *8*, 520–531.
- [46] M. Krummen, S. Balkow, L. Shen, S. Heinz, C. Loquai, H. C. Probst, S. Grabbe, *J. Leukocyte Biol.* **2010**, *88*, 189–199.

Received: June 12, 2014

Published online on August 8, 2014